

# A spiking network for body size learning inspired by the fruit fly

Paolo Arena, Giuseppe Di Mauro, Tammo Krause, Luca Patané and Roland Strauss

**Abstract**—The concept of peripersonal space is an interesting research topics for psychologists, neurobiologists and for robotic applications. A living being can learn the representation of its own body to take the correct behavioral decision when interacting with the world. To transfer these important learning mechanisms on bio-robots, simple and efficient solutions can be found in the insect world. In this paper a neural-based model for body-size learning is proposed taking into account the results obtained in experiments with fruit flies. Simulations and experimental results on a roving platform are reported and compared with the biological counterpart.

## I. INTRODUCTION

**T**He multisensory representation of our body (i.e. body schema), and its conscious and manipulable counterpart (i.e. body image) play a pivotal role in the development and expression of many higher level cognitive functions [1]. Two distinct and complementary definitions of such representation do exist: the body schema, an unconscious neural map of the spatial relations among the different body parts, where multi-modal sensory information (e.g. visual, somatosensory, and tactile) is integrated, and the body image, a consciously manipulable and body-centered version of the body schema used to form our perceptual, conceptual or emotional judgments towards our body [2], [3].

As robotic systems become more complex and versatile or are even delivered in a completely reconfigurable way, there is a growing demand for techniques allowing a robot to automatically learn body schemata with no or only minimal human intervention [4].

Key elements of this process are the plasticity of body representations (i.e. development, adaptation, extension), coordinate transformations, and the relationship between body schema and forward models. We can consider the body model as a sensorimotor representation of the body used for specific actions; it would encompass both *short-term* (e.g., position of a limb at a given instant) and *long-term* dynamics (e.g., biomechanical properties and size of limbs) [5].

The mental processes that lead to the formation of a body scheme involve a kind of adaptive calibration of an individual proprioceptive information to define a mental representation of its own body distinct from other individuals. This is achieved by detecting the causal effects between the self-produced contingent activity of the own actions and the induced sensory information (e.g., spatial position, somatosensory or visual or sonorous information) [6]. In humans, the construction of peripersonal space (i.e. the reach

of our hands and the step size of our legs) is developed by the visual feedback we get performing actions in the environment.

These mechanisms that seem to reside only in highly evolved and skilled animals can be identified also in the insect world. In particular, in *Drosophila melanogaster*, the simplest form of a body model is envisaged looking at the recent experiments in which genetically identical flies can experience differences in their body size of up to 15% due to environmental influences (e.g. food and temperature regime during the larval stages). Visual feed-back (parallax motion) from locomotion is required to calibrate the memory for the individual body size [7]. In gap climbing experiments with flies of different body sizes, the number of unsuccessful attempts was always maximum at the largest just surmountable gap width. This result allowed to assert that flies take into account their body size while taking behavioral decisions. Moreover, if flies hatched and lived in the dark, the body size is no more taken into account in the decision process.

Using the experimental results available, a neural model is here proposed based on the mechanisms used by flies to learn its body capabilities. The architecture has been applied to a simulated *Drosophila* in a scenario where the robot should learn through a reward based system the reachable/unreachable space in the arena.

## II. BODY SIZE IN DROSOPHILA: BIOLOGICAL EVIDENCES

Besides its tiny brain, *Drosophila melanogaster* shows a multitude of interesting behaviors and learning capabilities.

The body size, important information used to take decisions, is identified by flies using multisensory integration strategies: they need to connect visual input with tactile experience. Experiments performed to unravel the construction mechanisms demonstrate that flies, living in the dark since hatching, are less able to judge their capabilities than other flies raised in standard light-dark cycles.

It seems that the formation of this knowledge of the own body size needs that the fly is able to walk and generate parallax motion, by that shifting the retinal images of objects in the environment. The average step size of an individual [8], which is proportional to its leg length and therefore to the body size [9], will create an average parallax motion.

Ongoing experiments demonstrate that flies, living in the dark, are not able to correctly judge their own dimensions, until they are allowed to walk in light for some time. The body size memory formation seems to be based on a scaling of the step length using the parallax motion generated on the retina during locomotion. The training time is very short: ten to fifteen minutes with sufficient visual contrasts in the environment are enough to scale step length. Working

Paolo Arena, Giuseppe Di Mauro and Luca Patané are with the Dipartimento di Ingegneria Elettrica, Elettronica e Informatica, Università degli Studi di Catania, Italy (email: {parena, lpatane}@dieei.unict.it). Roland Strauss and Tammo Krause are with the Institut für Zoologie III (Neurobiologie), University of Mainz, Germany (email: rstrauss@uni-mainz.de

with learning mutant flies a mapping of the body size was performed and the key role of the central complex is being studied [10], [11].

In contrast to humans, flies have no need to re-adjust their peripersonal space because once enclosed they do not change their body size. But we can think to a more general body model where either changes in the payload or body structure modifications due to injuries can produce an adaptation of the internal model to match the new body configuration acquired interacting with the environment.

### III. MODEL FOR LEARNING BODY SIZE

Starting from the neurobiological data acquired from *Drosophila melanogaster* and having an implementation for robotic applications in mind, a neural model for body size learning using parallax information is proposed here, implemented and applied in a dynamic simulation environment using a fly-inspired legged robot. The fly model is able to walk in an empty arena with a single object placed in the center. After a transient needed to stabilize the locomotion gait in the legged structure, the robot proceeds in forward walking until the object is detected for the first time ( $t_1$  in Fig. 1). The information about the object position in the visual field is acquired through an uniformly distributed ring of neurons that have a one-to-one match with the insect ommatidia (about  $4.6^\circ$  each). The output of the stimulated neuron is modulated with a post synaptic weight that corresponds to the sinusoidal function of the angular position of the neuron as illustrated in Fig. 1. After a given number of steps (four steps have been considered in the following experiments) the robot evaluates the new angular position of the object ( $t_2$  in Fig. 1). The second acquisition is needed to evaluate the distance between the robot and the object through parallax: parallax is a displacement or difference in the apparent position of an object viewed along two different lines of sight. The mathematical formulation is reported in the following equation:

$$d_2 = \frac{\sin(\alpha)}{\sin(\delta - \alpha)} d_1 \quad (1)$$

where  $\alpha$  and  $\delta$  are the angular positions of the target acquired at time  $t_1$  and  $t_2$  by the robot,  $d_1$  is the distance traveled between the two acquisitions and  $d_2$  is the final distance between the robot and the target (see Fig. 2).

Starting from this mathematical formulation, a neural-based network has been designed and implemented obtaining similar results with spiking processing mechanisms. A complete block scheme of the proposed model is reported in Fig. 3.

The information on the object position acquired in two different time steps, is discretized and weighted as shown in Fig. 1. An array of class I Izhikevich's neurons is then used to evaluate the ratio between the two acquired sinusoidally modulated inputs. The equations of the adopted neural model are:

$$\begin{aligned} \dot{v} &= 0.04v^2 + 5v + 140 - u + I \\ \dot{u} &= a(bv - u) \end{aligned} \quad (2)$$

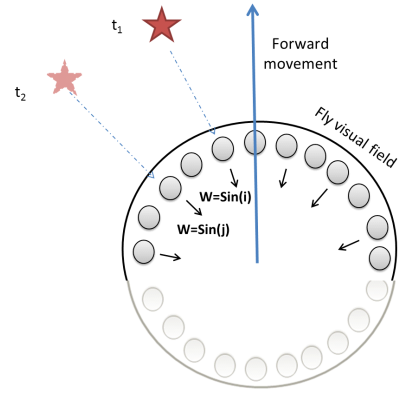


Fig. 1. Scheme of the acquisition of the object angular position in the fly visual field. At the time instant  $t_1$  the object is identified for the first time at the angular position  $i$  whereas after a given number of steps performed by the fly model in a straight forward direction the object will be visible at an instant  $t_2$  in a new angular position  $j$ . The weights associated to the neuron activity are shaped with a sinusoidal function depending on the position in the visual field.

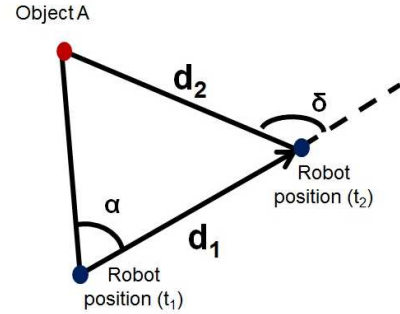


Fig. 2. Geometric relations between the detected object A and the robot that is moving forward with a fixed heading from position  $t_1$  to  $t_2$ .

with the spike-resetting

$$\text{if } v \geq 0.03, \text{ then } \begin{cases} v \leftarrow c \\ u \leftarrow u + d \end{cases} \quad (3)$$

where  $v$  is the membrane potential of the neuron,  $u$  is a recovery variable and  $I$  is the synaptic current that is constituted by a bias  $I_{bias}$ , a threshold current  $I_A$  and the input currents due to the topological connections  $I_{input}$ . The value used for the parameters are  $a=0.02$ ,  $b=-0.1$ ,  $c=-55$ ,  $d=6$ .

Each neuron is inhibited by the output of the neuron activated at time  $t_1$  and excited by the neuron activated at  $t_2$ . An array of gains is used to weight the second input to find the correct matching: excitatory inputs should compensate the inhibitory ones to allow the neuron firing. A bias current was added ( $I_{bias} = 82nA$ ) making each neuron able to fire with a minimal additional input current. A series of time delays ( $\tau_i$ ) was included to evaluate the neuron response in sequence. Each neuron is connected with the others with inhibitory synapses forming a winner-takes-all network topology.

The first active neuron (i.e. winning neuron) strongly

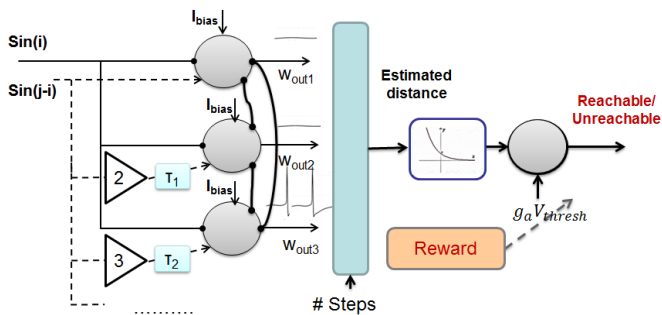


Fig. 3. Scheme of the implementation of the distance estimation through parallax with a spiking-based network. The first part of the processing stage is needed to evaluate the distance from the detected object in terms of number of steps whereas the last neuron is subject to a reward-based learning that, through a threshold adaptation mechanism, identifies the reachable space of the moving agent.

inhibits the others and produces an output proportional to its corresponding gain factor. Assuming that the system knows the distance traveled between the two time instants of acquisition (e.g. in terms of number of steps) the outcome of the first part of the network is a signal proportional to the object estimated distance. The last processing stage consists of a spiking neuron subject to a threshold adaptation learning process. Depending on a reward signal provided to the system, the threshold level is adapted either to facilitate or to reduce the spiking response of the neuron.

Threshold adaptation has a solid biological background: in fact, it can be seen as a consequence of the nonlinearities present in the neuron membrane dynamics [12]. Input-output functions adaptations for auditory neurons involved in sound coding were accurately detected and studied [13]. Moreover this mechanism seems to produce emergent cooperative phenomena in a large population of neurons, and seems to be responsible for contrast adaptation [14], [15], or for the scaling adaptation to varying stimuli in somatosensory cortex [16].

The threshold adaptation process can be modeled as a voltage-dependent current ( $I_A$ ) introduced as an additional input to the decision neuron, that can be expressed as  $I_A = -g_A V_{thresh}$ , defining  $g_A$  as an activation-conductance. The current can be modified to hyperpolarize or depolarize ( $I_A \rightarrow I_A \pm \Delta I_A$ ) neurons.

The output neuron acts as a gate: its firing activity is associated to reachable objects whereas a silent state corresponds to unreachable ones.

#### IV. SIMULATION RESULTS

The proposed parallax-based body size model has been used with a simulated *Drosophila*-inspired robot as shown in Fig. 4. The robot is randomly placed in an arena where an object of interest is positioned in the center. During the learning phase the system evaluates the distance from the target using the computational model previously discussed. The decision neuron will provide a prediction of reachability/unreachability that has to be verified by the robot.

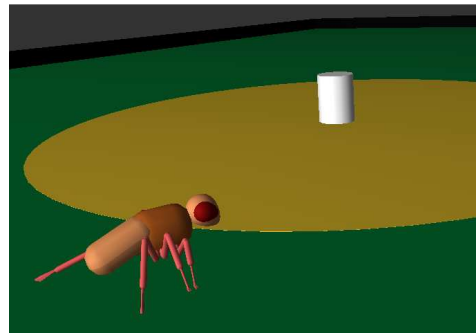


Fig. 4. Simulated *Drosophila*-inspired legged robot realized on a dynamic simulation environment.

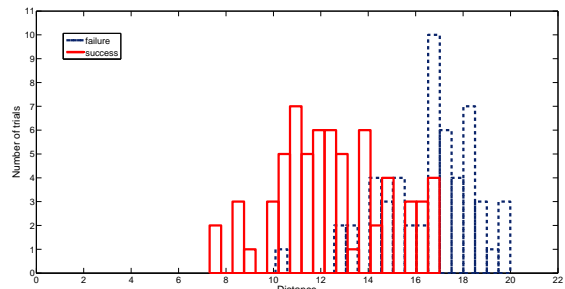


Fig. 5. Distribution of the final results in terms of successes and failures in an experiment where the robot is placed at different distance from the object of interest. The reward is provided if the object is reached within 15 steps.

At the beginning every object is assumed to be reachable and each trial the robot walks towards the target a reward is provided if it is reached within 15 steps. The reward activates the threshold adaptation mechanism: the threshold is modified depending on the coherence between the reinforcement signal and the internal prediction provided by the network. If the prediction is correct the threshold remains unchanged, otherwise, if the robot considers the object reachable (unreachable) but during the attempt the prediction is not confirmed, the threshold is increased (decreased) to hyperpolarize (depolarize) the output neuron. The learning process is summarized in the following equation:

$$V_{th} = \begin{cases} V_{th} + \Delta V_{th} & \text{for uncorrect attempt} \\ V_{th} & \text{for correct prediction} \\ V_{th} - \Delta V_{th} & \text{for uncorrect give up} \end{cases} \quad (4)$$

In the simulations the initial value used is  $V_{th} = 0$  and  $\Delta V_{th} = 0.5$ .

Fig. 5 shows the distribution of successes and failures in reaching an object located at different distances from the robot. The distribution of the starting positions that have been either rewarded or not rewarded is reported in Fig. 6. The attractive object is placed at the origin of the axis. A reduced set of the corresponding approaching trajectories followed by the robot is reported in Fig. 7.

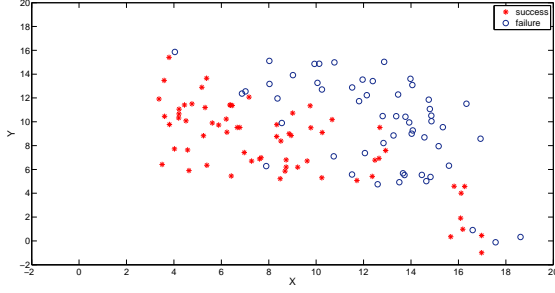


Fig. 6. Distribution of the starting positions from which the robot reached a success or a failure (a reward is given if the object, placed in (0,0), is reached in no more than 15 steps.

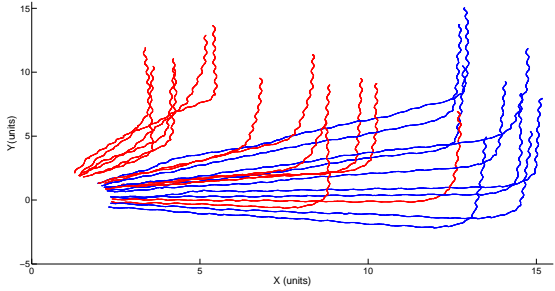


Fig. 7. Typical trajectories followed by the robot while reaching the target.

The time evolution of  $V_{th}$  for a learning experiment is shown in Fig. 8. The steady state value is related to the reachable distance learned by the robot.

As introduced in the biological experiment description, we performed simulations changing the body size of the simulated *Drosophila*. For sake of simplicity, we modified the step length by changing a parameter of the CPG-based locomotion control structure used to set the maximum angular excursion of the coxa joint [17], [18]. Therefore we considered a smaller fly (gain = 0.8), a standard fly (gain = 1) and a bigger fly (gain = 1.2).

A comparison with the biological experiments proposed for *Drosophila* has been performed evaluating the fraction of unsuccessful attempts as a function of the distance between robot and target (see Fig. 9). The simulations were performed in three different cases, changing the gain of the coxa joints for all the legs, thus allowing the robot to modify its step length. As shown in fly experiments performed in the gap climbing scenario, also in our model the peak of unsuccessful attempts is in correspondence with the maximum manageable distance and each system learns a different body size/peripersonal space.

To better analyze the behavior of the simulated fly, an extended statistical analysis has been performed evaluating, depending on the real distance between robot and target, the possible choices: successful and unsuccessful attempts, correct and incorrect give up. The results obtained in the three examined cases are reported in Fig. 10.

Finally the parallax evolution and its integration with the

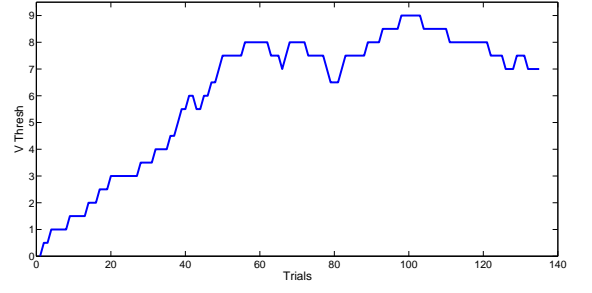


Fig. 8. Time evolution of the adaptive threshold tuned on the output neuron via a reward-based learning. The threshold stabilizes to a value that defines the reachability space of the robot.

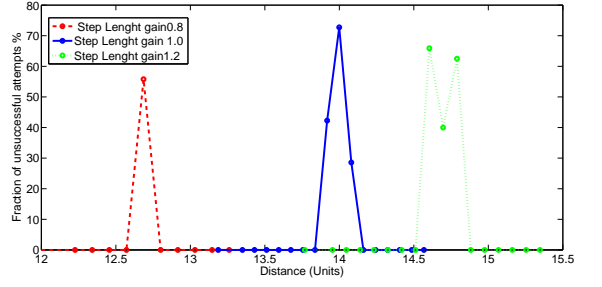
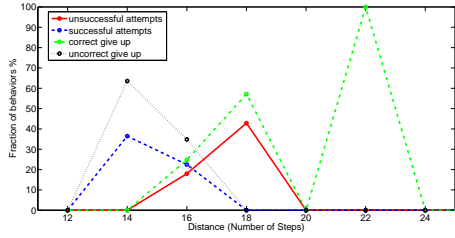


Fig. 9. Comparison between the behavior of the robot in three different cases where the amplitude of the coxa movement assumes the value  $A = [0.8, 1, 1.2]$ . The fraction of unsuccessful attempts is shown as a function of the distance between robot and target.

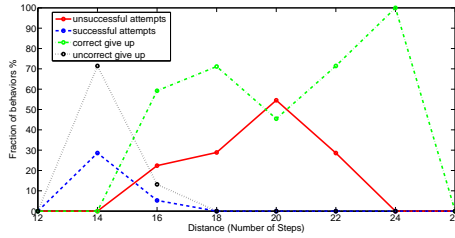
tactile information needed to evaluate the number of steps performed, can be artificially modulated through either visual compensation or a visual emphasis. To test the behavior of the network in these scenarios a moving target has been considered. To compensate or emphasize the effect of the parallax motion, a moving target with the same speed as the robot in the same direction (parallax compensation) and in the opposite direction (parallax emphasis) was considered. The threshold evolution is shown in Fig. 11 (a) and Fig. 12 (a): it can be noticed that  $V_{th}$  reaches the upper and lower saturation levels, respectively, and thus the robot considered the target always unreachable Fig. 11 (b) or reachable Fig. 12 (b). In fact in the first case the robot does not make attempts at all, whereas in the second case give-up decisions are missing.

## V. ROBOTIC EXPERIMENTS

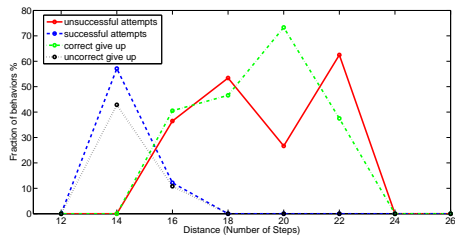
Following the interesting results obtained in the dynamic simulation environment, the proposed network was tested on a roving platform. The robot is actuated by four dynamixel RX28 servomotors, controlled by a microcontroller-based board. It is also equipped with a compass sensor, used for closed loop turning maneuvers, two sonars used for obstacle avoidance, two color sensors placed in the bottom part, used to detect landmarks on the ground, and an omni-directional camera. A netbook on board is used to host the high level control algorithm.



(a)



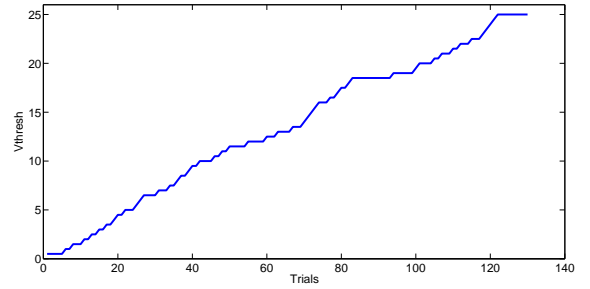
(b)



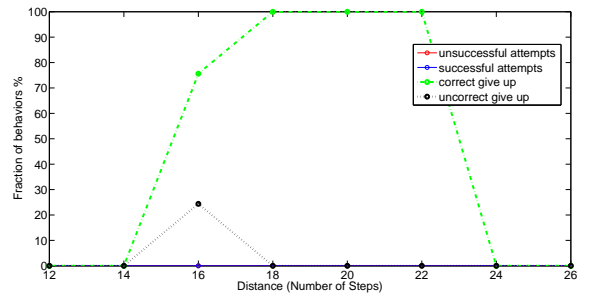
(c)

Fig. 10. Behavioral response, obtained over 200 testing trials, of the simulated *Drosophila* with body size reduced by 20% (a), standard (b) and increased by 20% (c).

The same learning procedure used in simulation was performed with the roving robot. The robot is initially placed in a starting position near a wall of a  $3 \times 2 \text{ m}^2$  arena. A monitor in the opposite side of the arena displays a white circle on a black background, used as target as depicted in Fig. 13. The home position, as well as the target position, are identified with colored landmarks on the ground. The robot, after a self-calibration procedure performed by the camera, acquires the angular position of the centroid of the detected target and, after a fixed forward movement of 30 cm, it acquires the new angular position. Using the procedure reported above, the robot estimates the distance and proceeds with a targeting behavior. A reward is provided if the target is successfully reached within 160 cm. Typical trajectories followed by the robot during learning are reported in Fig. 14. To start a new trial the robot comes back home and repeats the procedure. Due to position errors accumulated during the movements, the initial position changes each trial.



(a)

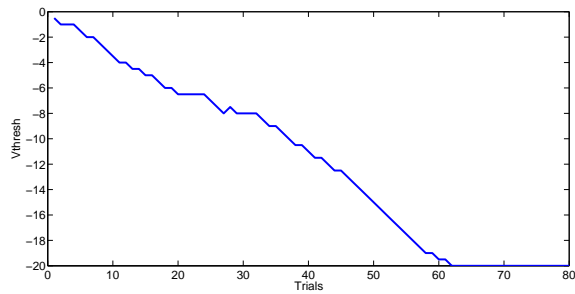


(b)

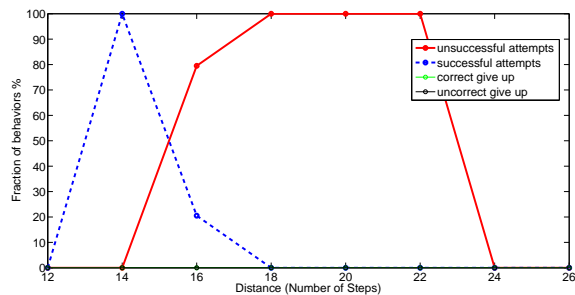
Fig. 11. Simulation with parallax emphasis: robot and target are moving with the same speed one toward the other. (a) Temporal evolution of the threshold during learning, (b) behavioral response of the robot during the testing phase.

A complete analysis of the robot behavior is shown in Fig. 15 where the results of the testing phases considering three different body sizes are reported, as already discussed for the dynamic simulations. It can be noticed that the level of unsuccessful attempts and incorrect give-up behaviors is lower in the robot experiment than in the simulated version. These results can be explained considering that the simulated legged system introduces in the estimation procedure a larger error than the roving platform. The high level of uncertainty obtained with simulated flies are also in line with the biological results obtained in the gap climbing scenarios.

Finally also in the robotic set-up the visual information has been altered either by emphasizing or compensating the parallax motion. The results reported were obtained using a series of adjacent monitors where the visual target can be moved depending on the robot actions. The results reported in Fig. 16 refer to a parallax emphasis which produces a continuous growth of the threshold level, and a completely compensated parallax: in this latter case the robot learns that every target is within its peripersonal space and always attempts to reach it; no give up behaviors are elicited, as expected.



(a)



(b)

Fig. 12. Simulation with parallax compensation, robot and target are moving with the same speed in the same direction. (a) Temporal evolution of the threshold during learning, (b) behavioral response of the robot during the testing phase.



Fig. 13. Roving robot used as testbed in an arena where visual targets are displayed on a monitor.

## VI. CONCLUSIONS

The capability of learning its own body dimensions is a crucial element for living beings and a very important demand for modern robotic systems. Looking into biology, even simple insects like *Drosophila* can learn to adapt their behaviors depending on their body size. Following this evidence a computational model based on spiking neurons and threshold adaptation learning mechanisms was developed and tested both in a simulated legged robot and in a real roving platform. The results demonstrate the capability of the system to learn how to shape its behaviors depending

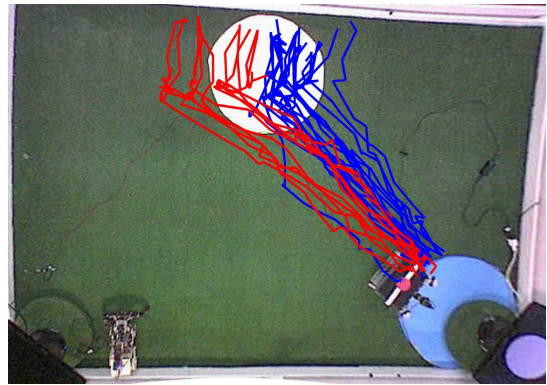


Fig. 14. Trajectories followed by the robot during the trials. The reward signal is provided to the robot depending to the distance covered to reach the target. The blue trajectories represent rewarded trials whereas the red ones are punished cases.

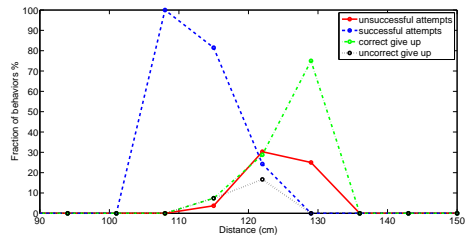
on its body size. Interesting results were also provided by artificially altering the visual perception of the robot either by emphasizing or compensating the parallax, by moving the visual target. The learning procedure, here applied to a targeting task, can be extended to other tasks like gap climbing and obstacle overcoming: these can be improved taking into account information on the body size of the system.

## ACKNOWLEDGEMENT

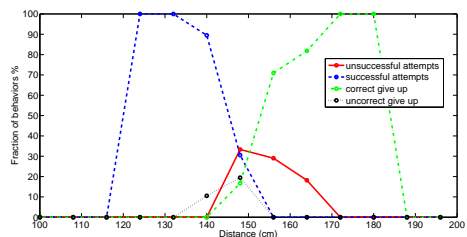
This work was supported by EU Project EMICAB, Grant N 270182.

## REFERENCES

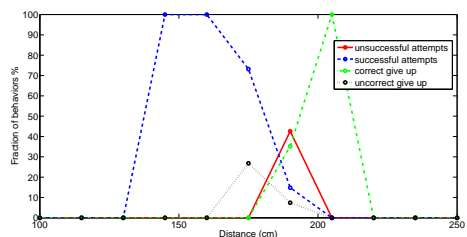
- [1] C. Nabeshima, M. Lungarella, and Y. Kuniyoshi, "Timing-based model of body schema adaptation and its role in perception and tool use: A robot case study," in *4th IEEE International Conference on Development and Learning (ICDL-05)*, pp. 7–12.
- [2] F. de Vignemont, "Body schema and body imagepro and cons," *Neuropsychologia*, vol. 48, no. 3, pp. 669–680, 2010.
- [3] S. Gallagher, *How the Body Shapes the Mind*. London, U.K.: Oxford Univ. Press, 2005.
- [4] J. Sturm, C. Plagemann, and W. Burgard, "Adaptive body scheme models for robust robotic manipulation," in *RSS - Robotics Science and Systems IV*, 2008.
- [5] M. Hoffmann, H. Marques, A. Hernandez, H. Sumioka, M. Lungarella, and R. Pfeifer, "Body schema in robotics: a review," *Autonomous Mental Development*, vol. 2, no. 4, pp. 304–324, 2010.
- [6] A. Pitti, H. Mori, S. Kouzuma, and Y. Kuniyoshi, "Contingency perception and agency measure in visuo-motor spiking neural networks," *IEEE Transactions on Autonomous Mental Development*, vol. 1, no. 1, 2009.
- [7] T. Krause and S. R., "Mapping the individual body-size representation underlying climbing control in the brain of *Drosophila melanogaster*," in *Proc. 33rd Gttingen Meeting of the German Neuroscience Society*, 2011, pp. T25–11B.
- [8] R. Strauss and M. Heisenberg, "Coordination of legs during straight walking and turning in *Drosophila melanogaster*," *J Comp Physiol A*, vol. 167, pp. 403–412, 1990.
- [9] D. Ben-Zvi, G. Pyrowolakis, N. Barkai, and B. Shilo, "Expansion-repression mechanism for scaling the dpp activation gradient in *Drosophila* wing imaginal discs," *Curr. Biol.*, vol. 21, no. 16, pp. 1391–1396, 2011.
- [10] R. Strauss, "The central complex and the genetic dissection of locomotor behaviour," *Curr. Opin. Neurobiol.*, vol. 12, pp. 633–638, 2002.
- [11] U. Hanesch, K. Fischbach, and M. Heisenberg, "Neuronal architecture of the central complex in *Drosophila melanogaster*," *Cell Tissue Res.*, vol. 257, pp. 343–366, 1989.



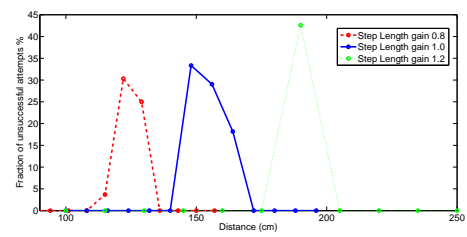
(a)



(b)

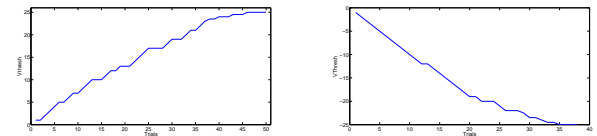


(c)

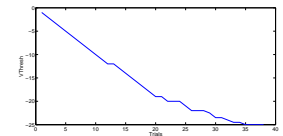


(d)

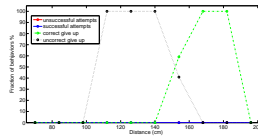
Fig. 15. Behavioral response, obtained over 100 testing trials, of the roving robot with body size reduced by 20% (a), standard (b) and increased by 20% (c). (d) Comparison between the unsuccessful attempts obtained in the three cases.



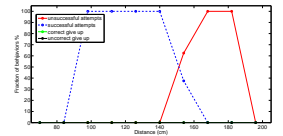
(a)



(b)



(c)



(d)

Fig. 16. Roving robot experiment with parallax emphasis and compensation, robot and target are moving with the same speed one toward the other or in the same direction. (a)-(b) Temporal evolution of the threshold during learning for emphasis and compensation respectively, (c)-(d) behavioral response of the robot during the testing phase

- [12] E. M. Izhikevich, "Which Model to Use for Cortical Spiking Neurons?" *IEEE Trans. on Neural Netw.*, vol. 15, no. 5, pp. 1063–1070, Sept. 2004.
- [13] I. Dean, N. S. Harper, and D. Mcalpine, "Neural population coding of sound level adapts to stimulus statistics," *Nature Neuroscience*, vol. 8, no. 12, pp. 1684–1689, Dec 2005.
- [14] V. Dragoi, J. Sharma, and M. Sur, "Adaptation-Induced Plasticity of Orientation Tuning in Adult Visual Cortex," *Neuron*, vol. 28, no. 1, pp. 287–298, Oct 2000.
- [15] M. W. Greenlee and F. Heitger, "The functional role of contrast adaptation," *Vision Research*, vol. 28, no. 7, pp. 791–797, 1988.
- [16] J. Garcia-Lazaro, S. Ho, A. Nair, and J. Schnupp, "Shifting and scaling adaptation to dynamic stimuli in somatosensory cortex." *European Journal of Neuroscience*, vol. 26, no. 8, pp. 2359–2368, Oct 2007.
- [17] E. Arena, P. Arena, and L. Patané, "CPG-based locomotion generation in a drosophila inspired legged robot," in *Biorob 2012*.
- [18] —, "Modelling stepping strategies for steering in insects," in *Frontiers in Artificial Intelligence and Applications vol. 234: Proceedings of the 21st Italian Workshop on Neural Nets*, pp. 275–283.